0026-895X/97/061095-10$3.00/0

MOLECULAR PHARMACOLOGY, **52:**1095–1104 (1997).

Voltage-Dependent Inhibition of N- and P-Type Calcium Channels by the Peptide Toxin ω-Grammotoxin-SIA

STEFAN I. McDONOUGH, RICHARD A. LAMPE, RICHARD A. KEITH, and BRUCE P. BEAN

Department of Neurobiology, Harvard Medical School, Boston, Massachusetts 02115 (S.I.M., B.P.B.), Vollum Institute, Oregon Health Sciences University, Portland, Oregon 97201 (S.I.M., B.P.B), and Department of Pharmacology, Zeneca Pharmaceuticals Group, Zeneca Inc., Wilmington, Delaware 19897 (R.A.L., R.A.K.)

Received June 5, 1997; Accepted August 16, 1997

SUMMARY

We studied the mechanism by which the peptide ω-grammotoxin-SIA inhibits voltage-dependent calcium channels. Grammotoxin at concentrations of >50 nM completely inhibited inward current carried by 2 mM barium through P-type channels in rat cerebellar Purkinje neurons when current was elicited by depolarizations up to +40 mV. However, outward current (carried by internal cesium) elicited by depolarizations to >+100 mV was either unaffected or enhanced in the presence of toxin. Tail current activation curves showed that grammotoxin shifted the steady state voltage dependence of channel activation by ≈+40 mV. Activation in the presence of toxin was far slower in addition to having altered voltage dependence. Grammotoxin also inhibited N-type calcium channels in rat and frog sympathetic neurons, with changes in channel voltage dependence and kinetics nearly identical to those of P-type channels. Experiments with monovalent ions as the only charge carriers showed that toxin effects on channel activation and kinetics depended on voltage, not on direction of current flow or on the current-carrying ion. Repeated trains of large depolarizations relieved toxin inhibition, as if toxin affinity for activated channels were low. The effects of grammotoxin on gating of P-type channels are very similar to those of ω-Aga-IVA, but combined application of the two toxins showed that grammotoxin binding is not prevented by saturating binding of ω-Aga-IVA. We conclude that grammotoxin potently inhibits both P-type and N-type channels by impeding channel gating and that grammotoxin binds to distinct or additional sites on P-type channels compared with ω-Aga-IVA.

Drugs and toxins that interact with ion channels have been valuable aids to understanding both structure and function of various types of channels. Two broad classes of drugs and toxins affecting voltage-dependent channels can be distinguished: those that block channels by physically occluding the pore of the channel and those that alter the voltage-dependent gating of the channels. Molecules believed to act as pore blockers have been useful in helping to define regions of the channel molecules that form the outer region of the pore. Prime examples include scorpion toxin interaction with *Shaker* family potassium channels or with calcium-activated potassium channels (1–4) and tetrodotoxin interaction with voltage-dependent sodium channels (5–8).

Toxins that alter channel gating may be useful in making inferences about regions of channel molecules that move during gating. A number of such toxins that act on voltage-dependent sodium, calcium, and potassium channels are known. Sodium channel gating is modified by α and β peptide toxins from scorpion venom, peptides from sea anemone venom, and lipid-soluble toxins such as batrachotoxin and veratridine that are isolated from plants or poison frogs (9–12). These toxins act as sodium channel agonists and increase cell excitability by slowing inactivation or shifting the voltage dependence of channel activation to more negative potentials. Toxins that inhibit opening of channels by affecting gating are also known. ω-Aga-IVA, a peptide isolated from the venom of the funnel web spider *Agelenopsis aperta*, inhibits P-type calcium channels by altering the voltage dependence of gating so very large depolarizations are required for channel opening (13). Similarly, hanatoxin, a peptide isolated from tarantula venom, inhibits *drk1* potassium channels by shifting the voltage dependence of gating in the depolarizing direction (14).

ω-Grammotoxin-SIA is a 36-residue peptide isolated from the venom of the tarantula *Grammostola spatulata* (15) that has been found to inhibit both P- and N-type channels in cultured hippocampal neurons (16). We studied the mechanism by which grammotoxin inhibits P- and N-type calcium channels and found that the toxin acts by altering the voltage-dependence of the channel, not by blocking the pore. The effects of grammotoxin on P-type channel gating are very similar to those of the spider toxin ω-Aga-IVA, but unlike

This work was supported by National Institutes of Health Grant HL35034.

ABBREVIATIONS: ω-Aga-IVA, ω-agatoxin-IVA; HEPES, 4-(2-hydroxyethyl)-1-piperazineethanesulfonic acid; TEA, tetraethylammonium; EGTA, ethylene glycol bis(β-aminoethyl ether)-*N*,*N*,*N*′,*N*′-tetraacetic acid; SCG, superior cervical ganglion; V_h, midpoint of Boltzmann function.

ω-Aga-IVA, grammotoxin affected N- as well as P-type channels. Also, the addition of grammotoxin to P-type channels after complete inhibition by ω-Aga-IVA resulted in an additional, nearly additive, effect on the voltage dependence of activation. The results suggest that the toxin binding site is conserved between N- and P-type channels and differs from that of ω-Aga-IVA. The toxin binding site has high affinity when channels are in closed states and low affinity when channels are activated.

Experimental Procedures

Cell preparation. Purkinje neurons were isolated from the brains of 8–16 day-old Long-Evans rats as described previously (13, 17). Sympathetic neurons were isolated from superior cervical ganglia of 12–21-day-old rats or sympathetic ganglia of adult bullfrogs (18). Purkinje neurons and rat sympathetic neurons were used within 8 hr of dissociation, and bullfrog sympathetic neurons were used within 32 hr.

Electrophysiological methods. Currents through voltage-activated calcium channels were recorded using the whole-cell configuration of the patch-clamp technique (19). Patch pipettes were made from borosilicate glass tubing (Boralex; Dynalab, Rochester, NY), coated with Sylgard (Dow Corning, Midland, MI), and sometimes fire-polished. Pipettes had resistances of 0.5–2 MΩ when filled with internal solution. After establishment of the whole-cell recording configuration, the cell was lifted off the bottom of the dish and positioned in front of an array of 12 perfusion tubes made of 250-μm internal diameter quartz tubing connected by Teflon tubing to glass reservoirs.

Currents were recorded with an Axopatch 200A amplifier (Axon Instruments, Foster City, CA), filtered with a corner frequency of 5 kHz (four-pole Bessel filter), digitized (10 kHz) using a Digidata 1200 interface and pClamp6 software (Axon Instruments), and stored on a computer. Compensation (typically 80–95%) for series resistance (typically ≈2.5 times higher than the pipette resistance) was used. Only data from cells with uncompensated series resistance and current sufficiently small to give a voltage error of <5 mV were analyzed. Calcium channel currents were corrected for leak and capacitative currents by applying 300 μM $CdCl_2$ to block calcium channel current or by subtracting a scaled current elicited by a 10-mV hyperpolarization from −80 mV.

Solutions. Except where noted, the internal (pipette) solution consisted of 56 mM CsCl, 68 mM CsF, 2.2 mM $MgCl_2$, 4.5 mM EGTA, 9 mM HEPES, 4 mM MgATP, 14 mM creatine phosphate (Tris salt), and 0.3 mM GTP (Tris salt), pH 7.4, adjusted with CsOH. For experiments on Purkinje neurons, the standard external solution contained 2 mM $BaCl_2$, 160 mM TEA-Cl, and 10 mM HEPES, pH 7.4, with TEA-OH and with 0.6 μM tetrodotoxin to block outward cesium currents through sodium channels, 5 μM nimodipine to block L-type calcium channels, 1 μM ω-conotoxin GVIA to block N-type calcium channels, and 1 mg/ml cytochrome *c* to prevent adsorption of ω-Aga-IVA or grammotoxin to reservoirs or tubing. Experiments on sympathetic neurons omitted ω-conotoxin GVIA; experiments on frog sympathetic neurons used 2 mM $BaCl_2$; and those on rat sympathetic neurons used 5 mM $BaCl_2$. External solutions were exchanged in <1 sec by moving the cell between continuously flowing solutions from the perfusion tubes. Potentials reported are uncorrected for a liquid junction potential of −2 mV between the pipette solution and the Tyrode's solution in which the offset potential was zeroed before seal formation.

Synthetic grammotoxin was prepared in a 1-mM stock solution in H_2O, stored at −20°, and diluted in the external solution on the day of the experiment. Previous work has shown that synthetic grammotoxin has identical properties and potency as that purified from *G. spatulata* toxin (20). Synthetic ω-Aga-IVA was the kind gift of Dr. Nicholas Saccomano (Pfizer, Groton, CT).

To obtain better resolution of tail current kinetics, most experiments were done at 10–12°, with the chamber cooled by circulation of 3° water through copper tubing that cooled a copper plate under the chamber. Temperature was measured using a thermistor in the bath. Experiments of relief of inhibition by trains of depolarizations were done at room temperature (20–22°), where both relief and reestablishment of inhibition were markedly more rapid. Values are given as mean ± standard error.

Results

Inhibition of P-type calcium channels. Grammotoxin effectively inhibited inward current through P-type calcium channels activated by moderate depolarizations. Fig. 1 shows the effect of 50 nM grammotoxin on current elicited by a depolarization to 0 mV in a rat cerebellar Purkinje neuron studied with 2 mM barium (with 5 μM nimodipine to block L-type calcium channels and 1 μM ω-conotoxin GVIA to block N-type calcium channels). The time course of inhibition was described well by a single exponential function with a time constant of 22 sec. Fig. 2 shows the effect of grammotoxin on current elicited by depolarization to a wide range of voltages. Grammotoxin completely inhibited inward current carried by barium at voltages from −40 to +40 mV. Depolarizations positive to +70 mV elicited outward currents. These currents are carried by internal cesium through calcium channels because they were lacking when cesium was replaced by *N*-methyl-D-glucamine or TEA and were blocked by 600 μM $CdCl_2$. The outward currents elicited by depolarizations positive to +70 mV were not completely inhibited by grammotoxin; in fact, the current elicited by a step to +150 mV was actually larger (by ≈60%) after the application of grammotoxin. The inward tail current at −60 mV after the step to

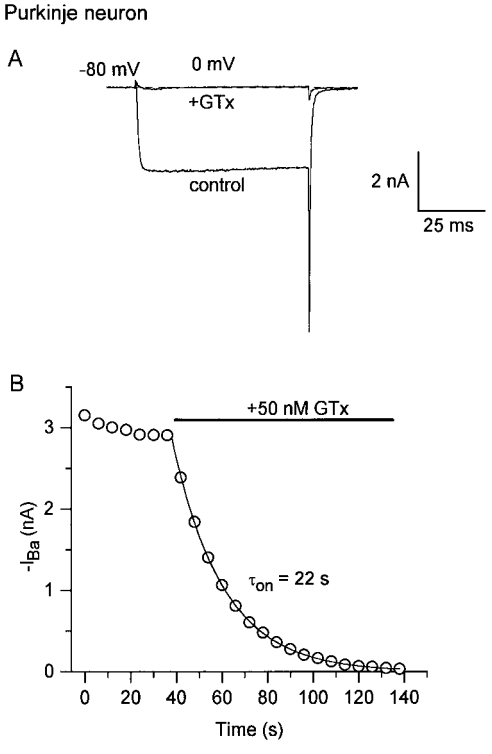

Fig. 1. Inhibition of P-type calcium channel current by 50 nM grammotoxin in a Purkinje neuron at 22°. A, Currents at 0 mV before and after grammotoxin (90-sec exposure). B, Time course of inhibition of test current.

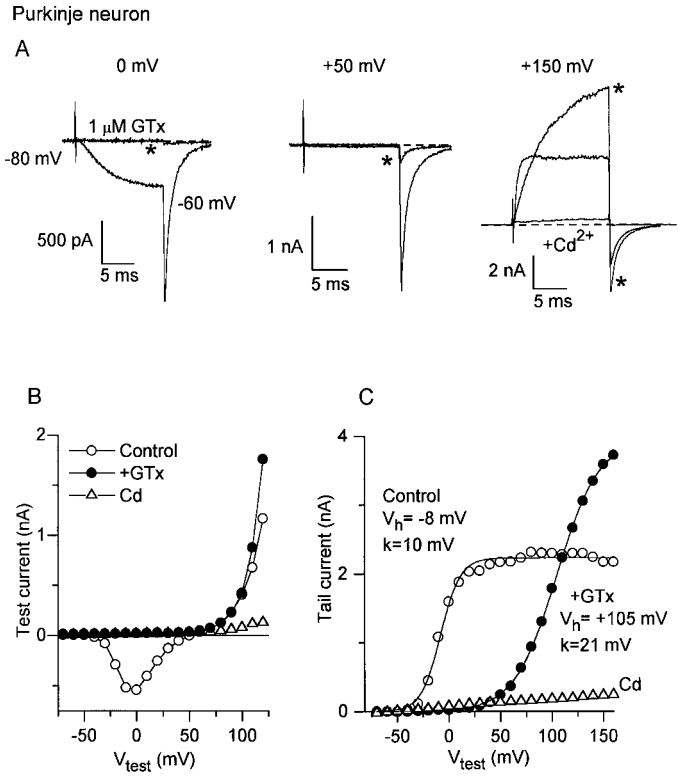

Fig. 2. Voltage dependence of P-type current before and after inhibition by 1 μM grammotoxin in a Purkinje neuron at 10°. A, Currents in response to 15-msec test pulses to voltages of 0, +50, and +150 mV before and after (*) inhibition by grammotoxin (*GTx*). *Cd* (at +150 mV), trace was taken after block by 600 μM Cd. B, Current measured at the end of the 15-msec test pulse in control and in grammotoxin (*GTx*) as a function of test voltage. C, Peak tail currents at −60 mV as a function of test voltage. *GTx*, grammotoxin. *Smooth curves*, fits to the Boltzmann function $I = I_{max}/\{1 + \exp[-(V - V_h)/k]\}$.

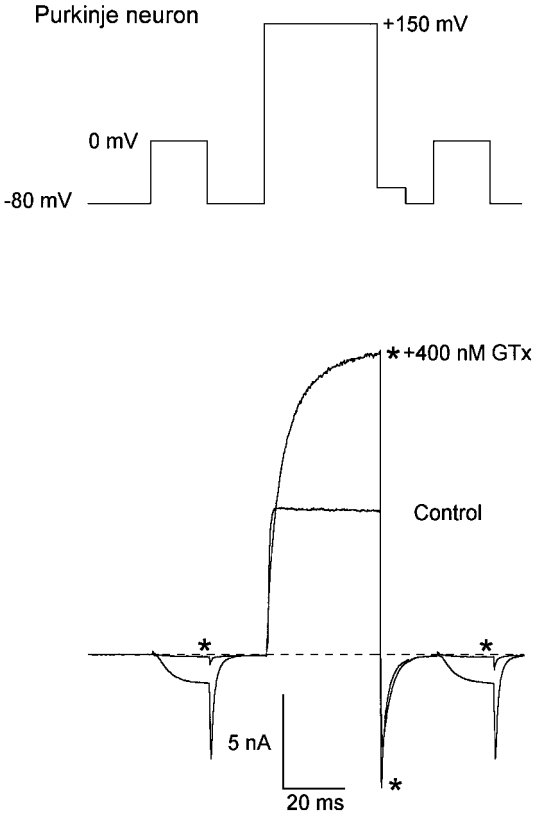

Fig. 3. Persistent grammotoxin inhibition of inward current after activation of large outward current in a Purkinje neuron at 10°. Outward current was evoked by a 40-msec step to +150 mV, bracketed by two 20-msec test pulses to 0 mV, before and after (*) inhibition by 400 nM grammotoxin (*GTx*).

+150 mV was also enhanced by grammotoxin. These effects are summarized by the plot of peak tail current versus test voltage (Fig. 2C). Grammotoxin apparently changes the voltage dependence of gating, so channels do not open in response to the moderate depolarizations that evoke inward current through unblocked channels; however, channels can still be maximally opened by sufficiently large depolarizations. In control, the tail current activation curve was fit by a single Boltzmann distribution with $V_h = -8$ mV and slope $k = 10$ mV. With grammotoxin, V_h increased to +105 mV, and the slope was more shallow ($k = 21$ mV). In collected results from six cells analyzed with this protocol, V_h increased from -14 ± 2 mV in control to $+97 \pm 4$ mV in grammotoxin, and k increased from 8 ± 1 mV in control to 26 ± 3 mV in grammotoxin. Maximal outward and tail current amplitudes were larger with toxin in three of six cells.

In principle, the slowly activating outward currents with grammotoxin could represent grammotoxin unbinding from the channel during large depolarizing pulses. To test whether grammotoxin was still bound to the channel after large depolarizations, a test pulse to 0 mV was given 20 msec after a 40-msec depolarization to +150 mV (Fig. 3). The current at 0 mV was still inhibited by grammotoxin after the depolarization to +150 mV, suggesting that grammotoxin was still bound to the channel. The rate of development of inhibition upon grammotoxin exposure occurred with a time constant of 17 sec for this cell (400 nM toxin at 10°), which is very slow compared with the 20-msec interval between the pulse to +150 mV and the start of the second pulse to 0 mV. Thus, it is far more likely that the inhibition during the second pulse to 0 mV reflects continuous presence of grammotoxin on the channel throughout the pulse sequence rather than toxin unbinding during the pulse to +150 mV followed by rebinding before the following pulse to 0 mV. Our interpretation is that the outward current at +150 mV reflects activation of toxin-bound channels with this strong depolarization.

The time course of activation of toxin-bound channels was studied at a variety of voltages by monitoring tail currents after test pulses of increasing durations. Fig. 4A shows currents elicited by steps to +90 mV incremented at 5-msec intervals in control and with grammotoxin. In control, activation was complete within 5 msec. With grammotoxin, the time course of activation could be fit well by a single exponential function with a time constant of 44 msec. The time constant of activation in toxin decreased from 117 msec at +30 mV to 7 msec at +180 mV (Fig. 4B). At voltages sufficiently far from the reversal potential to evoke clear outward currents, the time course of activation of outward current had a parallel time course with the growth of tail currents.

Although grammotoxin dramatically slowed activation kinetics, deactivation kinetics were affected much less. Fig. 4C shows tail currents at −60 mV after a 20-msec depolarization to +120 mV. The tail currents with and without toxin nearly superimpose, with fitted time constants of 2.6 msec for control and 2.4 msec for grammotoxin.

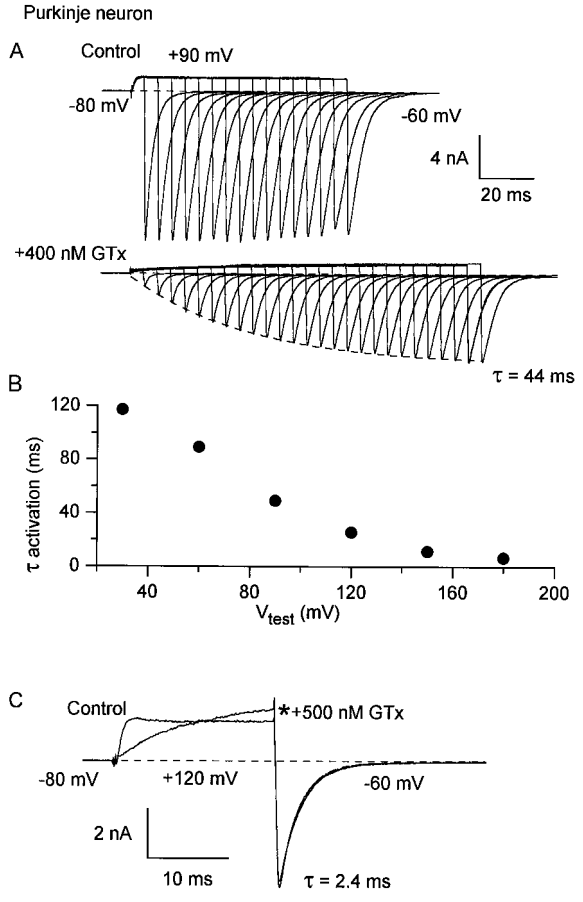

Fig. 4. Effects of grammotoxin (*GTx*) on channel activation and deactivation kinetics in Purkinje neurons at 10°. A, Tail currents at −60 mV in response to voltage steps to +90 mV in control and in the presence of 400 nM grammotoxin. With grammotoxin, current for a test pulse to −10 mV was monitored after each pulse to +90 mV to ensure grammotoxin had not unbound appreciably during the test pulse. Acquisition was paused for 4 sec between each test pulse to allow rebinding of any grammotoxin that had dissociated from the channel. A single exponential decay function is superimposed over the tail current envelope in grammotoxin. B, Activation time constant in grammotoxin as a function of voltage. C, Comparison of deactivation rates in control and in 500 nM grammotoxin (*). An exponential fit with $\tau = 2.4$ msec (*dashed line*) is added to the plot.

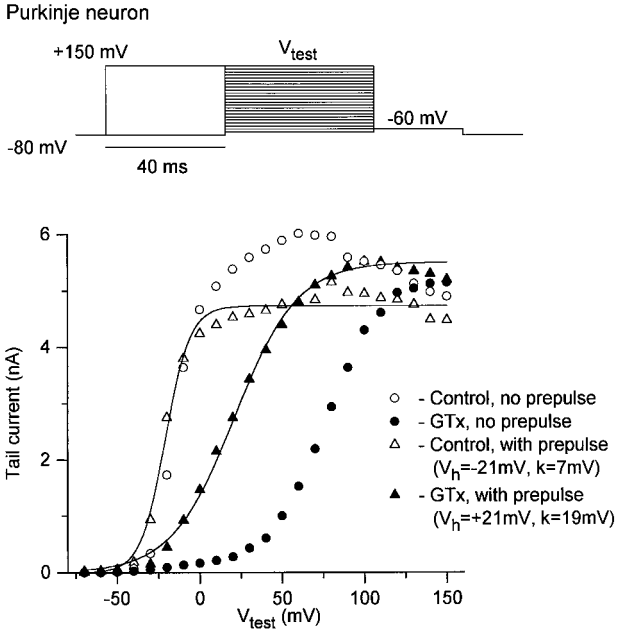

Fig. 5. Tail current activation curves in control and in grammotoxin (*GTx*), with and without a fully activating prepulse in a Purkinje neuron at 10°. Tail current at −60 mV is plotted as a function of test voltage. *Open symbols*, control currents. *Filled symbols*, currents with 400 nM grammotoxin. *Circles*, test voltage stepped directly from −80 mV. *Triangles*, test voltage preceded by a 40-msec prepulse to +150 mV. In grammotoxin, current at 0 mV was monitored after each test voltage to ensure that grammotoxin had not unbound appreciably. Acquisition was paused 4 sec between test pulses to allow rebinding of any grammotoxin that dissociated from the channel. Curves are single Boltzmann functions fitted to activation curves with the prepulse.

Because toxin-bound channels activate so slowly compared with normal channels, it is evident that steady state activation is not reached during the 15-msec test pulses used to define activation curves in Fig. 2. To better define steady state activation curves, we compared activation curves determined by 50-msec test steps delivered from −80 mV (starting with no activation) or after a 40-msec prepulse to +150 mV, which produces maximal activation in both the absence and presence of toxin. In control, the activation curve was not dramatically affected by the prepulse (Fig. 5). In the presence of toxin, the activation curve determined with the prepulse was shifted in the hyperpolarizing direction ($V_h = +21$ mV) compared with that determined without prepulse ($V_h = +75$ mV). The activation curves determined with prepulses probably approximate steady state voltage dependence because deactivation is rapid both in control and with toxin. In activation curves with prepulses, the activation curve in toxin is still much more positive than in control ($V_h = -21$ mV in control and +21 mV with toxin) and more shallow (slope factor $k = 7$ mV in control and 19 mV with toxin), although the difference in midpoint is much less than that with conventional protocols. In collected results from five cells with activation curves determined with prepulses, V_h averaged -17 ± 2 mV in control and $+23 \pm 3$ mV in toxin. The slope factor averaged 10 ± 1 mV in control and 20 ± 1 mV in toxin.

Recovery from grammotoxin inhibition on washout of toxin was slow and incomplete when assayed by moderate test pulses, but recovery was dramatically accelerated by repetitive strong depolarizations; this effect is illustrated in Fig. 6. Inhibition and recovery were monitored by test pulses to −20 mV (Fig. 6, *top*). (Unlike Figs. 2–5, the experiments in Figs. 6 and 7 were done at room temperature, at which inhibition and recovery were faster than at 10°.) Inward current at −20 mV was reduced to zero by 200 nM grammotoxin. Recovery of current on washout of grammotoxin was slow, with ≈5% recovery after 1 min. When the voltage protocol was altered so the test pulse to −20 mV was preceded by two 20-msec depolarizations to +150 mV, however (Fig. 6, ●), the recovery was complete within 1 min. The traces in Fig. 6 (*bottom*) show changes in the currents at −20 and +150 mV during inhibition and recovery; as inhibition at −20 mV was relieved, the outward currents at +150 mV decreased and the kinetics of activation at +150 mV became faster. The changes at −20 and +150 mV occurred with a parallel time course, which is consistent with both reflecting unbinding of toxin.

In the experiment reflected in Fig. 6, the depolarizations to +150 mV that seemed to accelerate unbinding of toxin elicited large outward current flow carried by cesium ions. How-

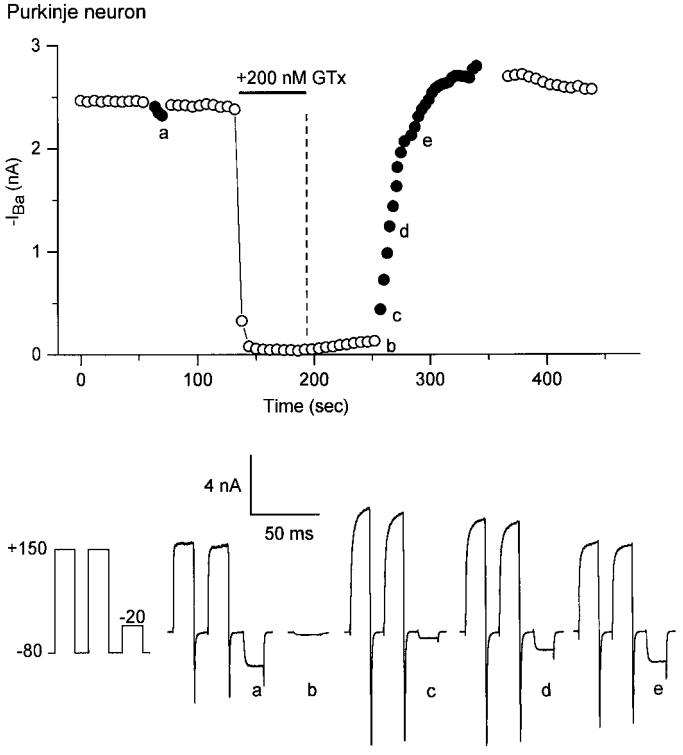

Fig. 6. Trains of large depolarizations speed recovery from grammotoxin inhibition in a Purkinje neuron at 22°. *Top*, time course of current measured with a 20-msec test pulse to −20 mV. ●, test pulse was preceded by two 20-msec pulses to +150 mV (*bottom left*, protocol). *Horizontal bar*, application of 200 nM grammotoxin. *Dashed vertical line*, washout of grammotoxin. *Bottom*, currents from the indicated points in the time course.

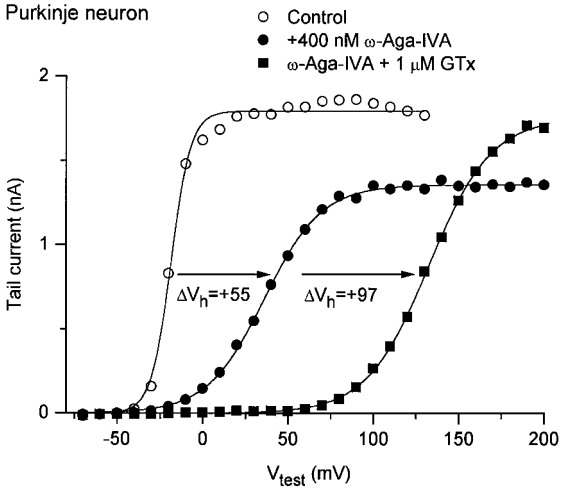

Fig. 7. Tail current activation curves in control, 400 nM ω-Aga-IVA, and 400 nM ω-Aga-IVA plus 1 μM grammotoxin (*GTx*) in Purkinje neuron at 10°. Tail currents at −60 mV were plotted as a function of test voltage. Solid curves are Boltzmann fits with parameters (V_h and k = −19 and 6 mV for control, +36 and 17 mV in ω-Aga-IVA, and +133 and 18 mV in ω-Aga-IVA plus grammotoxin).

ever, the outward current flow was not necessary for the effect. Depolarization to +150 mV accelerated recovery from inhibition equally well in experiments with TEA as the internal cation, in which there was no outward current. This suggests that strong depolarizations put the channel in a state for which grammotoxin has much lower affinity and that rapid unbinding occurs regardless of whether outward current flows.

The characteristics of grammotoxin inhibition of P-type channels are strikingly similar to inhibition by ω-Aga-IVA (13). Both toxins increase the half-maximal activation voltage, make the slope of the activation curve more shallow, slow the kinetics of channel opening, and dissociate more rapidly with strong depolarizations. To determine whether grammotoxin and ω-Aga-IVA bind to the same site on the channel, we tested whether grammotoxin binding was prevented by ω-Aga-IVA binding. This was facilitated by the larger effect of grammotoxin alone on the activation curve determined with a conventional protocol (midpoint shift of +110 mV) than of ω-Aga-IVA alone (+50 mV). Thus, if previous occupancy by ω-Aga-IVA prevented binding of grammotoxin to the same site, exposure to ω-Aga-IVA should prevent the additional shift expected from grammotoxin. Because it takes hours for ω-Aga-IVA to dissociate from P-type channels in the absence of trains of large depolarizations (17), it is unlikely that ω-Aga-IVA would be significantly replaced by grammotoxin over a time scale of even tens of minutes if both bound to the same site. Fig. 7 shows activation curves determined successively in control, after exposure to saturating ω-Aga-IVA, and after exposure to the combination of grammotoxin and ω-Aga-IVA. Grammotoxin caused a shift in the half-maximal activation voltage beyond that seen with ω-Aga-IVA alone. In fact, the shifts caused by grammotoxin and ω-Aga-IVA were nearly additive: ω-Aga-IVA shifted the midpoint by +55 mV and grammotoxin (in the continued presence of ω-Aga-IVA) shifted the midpoint by an additional +97 mV, not much less than the average shift of +111 mV seen with grammotoxin alone. The result is consistent with ω-Aga-IVA and grammotoxin binding to distinct sites that both produce a shift in activation but whose effects are nearly independent of one another. In combined results from three cells, grammotoxin increased V_h by +98 ± 6 mV after inhibition by ω-Aga-IVA. The slope factor was similar with ω-Aga-IVA alone (20 ± 2 mV) and with ω-Aga-IVA plus grammotoxin (24 ± 5 mV).

Inhibition of N-type calcium channels. Grammotoxin has been reported to block N-type calcium channels in rat dorsal root ganglion neurons (21) and cultured hippocampal neurons (16). We investigated whether the mechanism of inhibition is similar for both N- and P-type channels. Fig. 8 shows the effects of grammotoxin on current through N-type calcium channels in rat superior cervical ganglion neurons. As with P-type channels, grammotoxin inhibited completely both test pulse current and tail current for test pulses to voltages from −30 to +40 mV, but depolarizations beyond +50 mV still activated tail currents (the experiment depicted in Fig. 8 used TEA rather than cesium as the main internal cation, so there was no outward current for large depolarizations in control or with toxin). Tail current activation curves required a sum of two Boltzmann functions in control, which is consistent with a significant fraction of the channels being in the "reluctant" gating mode due to tonic modulation by G proteins (22–24). Fits to control currents from six cells gave V_h = −11 ± 0.5 mV, k = 8 ± 0.2 mV for the first Boltzmann function and V_h = +63 ± 10 mV, k = 31 ± 4 mV for the second Boltzmann function. In grammotoxin, curves were fit well by a single Boltzmann function with average values of V_h = +89 ± 1 mV and k = 21 ± 0.6 mV. Maximal tail current

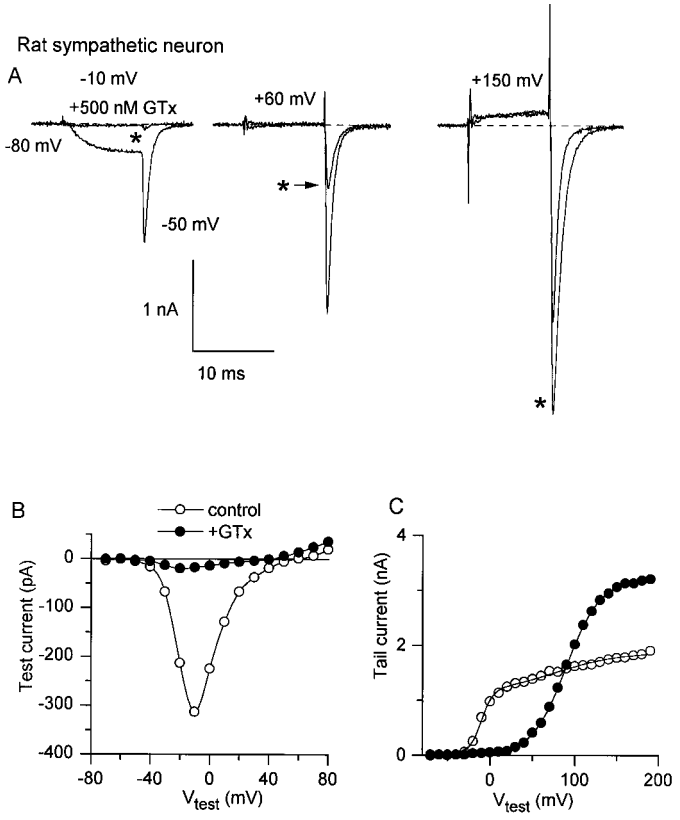

Fig. 8. Effect of 500 nM grammotoxin (*GTx*) on current through N-type calcium channels in a rat sympathetic neuron at 22°. A, Currents in response to 10-msec test pulses to the indicated voltage. *, Traces in grammotoxin. The internal TEA does not support outward currents. B, Test current as a function of test voltage. C, Peak tail current as a function of test voltage. *Smooth curve through control points*, sum of two Boltzmann functions, with V_h and k values of −10 and 7 mV and of +75 and 39 mV, respectively. *Smooth curve in grammotoxin*, single Boltzmann function, with V_h and k values of +89 and 20 mV. The external solution consisted of 160 mM TEA-Cl, 5 mM $BaCl_2$, 0.6 μM tetrodotoxin, 1 mg/ml cytochrome *c*, and 5 μM nimodipine. The internal solution consisted of 117 mM TEA-Cl, 9 mM HEPES, 9 mM EGTA, 4.5 mM $MgCl_2$, 4 mM MgATP, 14 mM creatine phosphate (Tris salt), and 0.3 mM GTP (Tris salt), pH 7.4 with TEA-OH.

was increased with grammotoxin in five of six SCG neurons, with an average increase of 60 ± 14% in those five.

It is striking that both for P- and N-type channels, the activation of channels in the presence of grammotoxin begins at +40–50 mV, which is close to the reversal potential for current flow through the channel. Is it just a coincidence that activation in toxin occurs near voltages where net current flow changes from divalent to monovalent current carrier and where current changes from inward to outward? We tested the possibility that the species of ion or direction of current flow influences the grammotoxin effect by examining the effect of toxin on currents through N-type channels with only monovalent ions traversing the channel from either side of the membrane. For this experiment, we recorded currents through N-type calcium channels in bullfrog sympathetic neurons, a preparation in which robust, stable monovalent currents can be obtained (25). Monovalent currents were recorded with 20 mM external sodium and 113 mM internal cesium; with these conditions, the reversal potential was −20 mV. The application of 1 μM grammotoxin effectively inhibited inward current carried by sodium ions at −30 mV and outward current carried by cesium ions at +30 mV (Fig. 9A). The result shows that grammotoxin can effectively inhibit outward current as long as the depolarization is not sufficiently strong to activate the toxin-bound channels and that currents carried by monovalent ions can be inhibited regardless of the direction of flow. As with divalent solutions, toxin shifted the activation curve determined for all monovalent currents in the depolarizing direction, and for sufficiently large depolarizations, tail currents reached or exceeded control values. The results are consistent with the idea that the voltage dependence of grammotoxin inhibition results from alteration of gating of the channel and not from the direction of current flow.

Just as for P-type channels, grammotoxin inhibition of N-type channels assayed with moderate depolarizations could be reversed rapidly with trains of large depolarizing pulses. We were able to examine in detail the voltage and time dependence of reversal using N-type channels from bullfrog sympathetic neurons, taking advantage of the fact that these neurons can withstand trains of strong depolarizations to very positive voltages. For the experiment shown in Fig. 10, currents were inhibited with 500 nM grammotoxin (*top left*), and the cell was returned to control solution. The cell

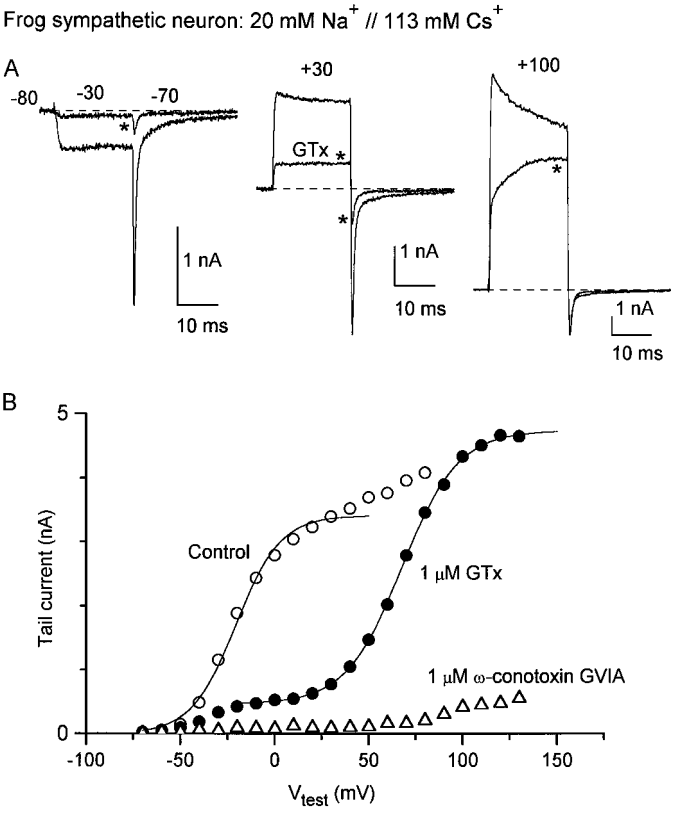

Fig. 9. Monovalent currents with and without 1 μM grammotoxin (*GTx*) in a bullfrog sympathetic neuron at 22°. A, Currents measured at test voltages of −30, +30, and +100 mV from a holding voltage of −80 mV, with tail currents measured at −70 mV. B, Tail currents as a function of test voltage in control, grammotoxin, and 1 μM ω-conotoxin GVIA. *Solid curves*, Boltzmann fits with V_h and k values of −21 and 12 mV in control and +68 and 15 mV in grammotoxin. The external solution consisted of 140 mM TEA-Cl, 10 mM HEPES, 20 mM NaCl, 1 mM EDTA, 2 μM nimodipine, 0.6 μM tetrodotoxin, and 1 mg/ml cytochrome *c*. The internal solution consisted of 113 mM CsCl, 4.5 mM $MgCl_2$, 9 mM HEPES, 9 mM EGTA, 14 mM creatine phosphate (Tris salt), and 0.3 mM GTP (Tris salt), pH 7.4, with CsOH.

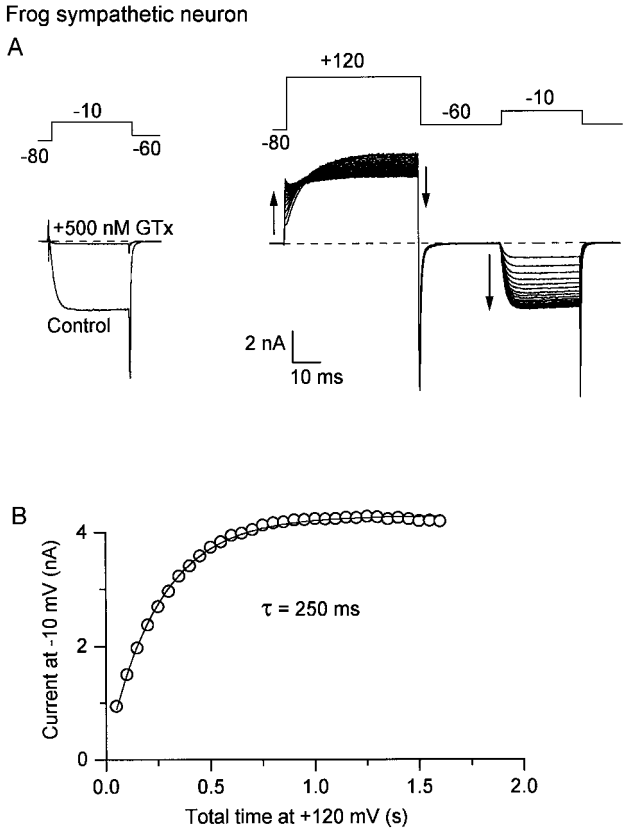

Fig. 10. Dissociation of grammotoxin (*GTx*) induced by successive strong depolarizations in a bullfrog sympathetic neuron at 22°. A, Current at −10 mV before and after inhibition by 500 nM grammotoxin (*left*) and progressive removal of the inhibition by pulses to +120 mV (*right*). *Superimposed traces*, 22 consecutive 50-msec pulses to +120 mV, followed by a 30-msec test pulse to −10 mV, delivered at 1 Hz. *Arrows*, direction of change in current with each successive pulse to +120. B, Current at −10 mV as a function of cumulative time at +120 mV (50 msec for each episode). Current magnitude is inverted for clarity. The fit is a single exponential function with time constant of 0.25 sec.

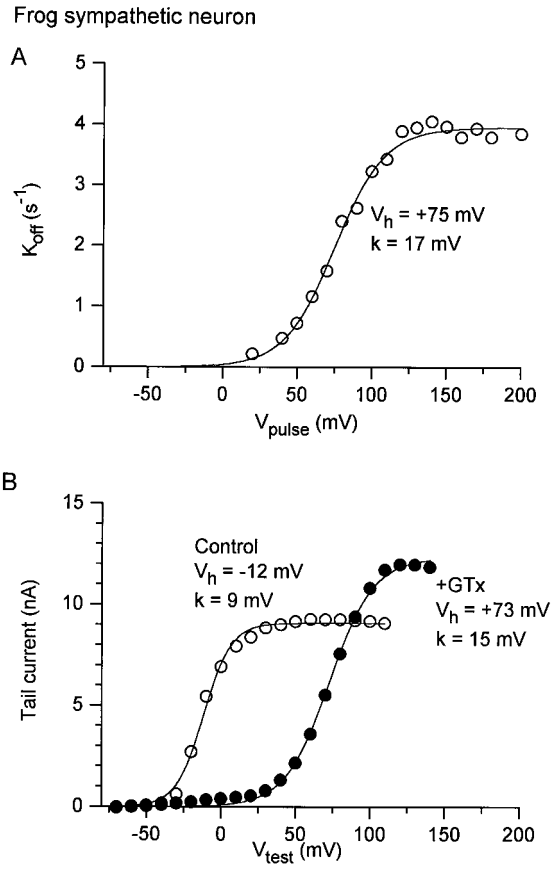

Fig. 11. Apparent off-rate of grammotoxin (*GTx*) compared with channel opening in grammotoxin as a function of voltage in a frog sympathetic neuron at 22°. A, Apparent off-rate of grammotoxin, obtained as in Fig. 10, as a function of voltage. Apparent off-rate is calculated as $1/\tau_{off}$ for each voltage. B, Tail current activation curves for the same cell in control and after inhibition by grammotoxin. Tail current at −60 mV was measured after 30-msec test pulses to the voltage indicated. Acquisition was paused for 2 sec between each episode to allow rebinding of any grammotoxin that had dissociated during a depolarizing test pulse. The external solution consisted of 160 mM TEA-Cl, 10 mM HEPES, 2 mM $BaCl_2$, 0.6 μM tetrodotoxin, 1 mg/ml cytochrome *c*, and 5 μM nimodipine, pH 7.4 with TEA-OH. The internal solution consisted of 113 mM CsCl, 4.5 mM $MgCl_2$, 9 mM HEPES, 9 mM EGTA, 14 mM creatine phosphate (Tris salt), and 0.3 mM GTP (Tris salt), pH 7.4, adjusted with CsOH. Grammotoxin was 500 nM.

then received 50-msec depolarizations to +120 mV, each followed by a test pulse to −10 mV, at 1 Hz (*top right, traces overlaid*). The inhibitory effects of grammotoxin were gradually removed: current at −10 mV increased, outward current at +120 mV decreased, and the kinetics of outward current quickened. Current at −10 mV as a function of the cumulative time at +120 mV was fit well by a single exponential function with a time constant of 250 msec (Fig. 10, *bottom*), corresponding to an off-rate $k_{off} = (250 \text{ msec})^{-1} = 4 \text{ sec}^{-1}$.

For the same cell, this procedure was used to calculate the off-rate at a variety of potentials. After each series of depolarizing trains had removed inhibition, grammotoxin was reapplied, and the inhibition was removed with depolarizations to a different voltage. In each case, the recovery from inhibition (determined by test pulses to −10 mV) was fit well by a single exponential function; the corresponding apparent off-rates are plotted in Fig. 11A. The apparent off-rate as a function of voltage could be fit well by a single Boltzmann function with $V_h = +75$ mV and slope $k = 17$ mV. For three cells studied with the same protocol, $V_h = 76 \pm 0.6$ mV and $k = 18 \pm 0.7$ mV. In each case, the apparent off-rate clearly saturated, at $k_{off} = 3.9 \pm 0.3 \text{ sec}^{-1}$. Tail currents as a function of test voltage for this cell are plotted in Fig. 11B, in control and in grammotoxin. The activation curve in toxin had values of $V_h = +73$ mV and $k = 15$ mV, which were very similar to the voltage dependence of the apparent off-rate. The precise agreement of midpoints is fortuitous because for both measurements, the midpoints would be expected to vary somewhat with pulse duration due to the slow activation of toxin-bound channels Nevertheless, the saturation of the apparent off-rate positive to +120 mV, at which channel activation in the presence of toxin also saturates, strongly suggests that the voltage dependence of the off-rate derives from the voltage dependence of channel gating and that toxin unbinds more rapidly from activated channels than from closed channels.

The voltage dependence of N-type calcium channel gating can be altered by G protein-coupled neurotransmitters (23, 24, 26–29). We tested whether grammotoxin prevented additional effects of G proteins. The addition of 200 nM somatosta-

tin to rat SCG neurons resulted in a shift of tail current activation curves to more depolarized potentials (Fig. 12), as shown previously (22, 23, 30). In recordings from eight cells, somatostatin inhibited the tail current after a step to 0 mV (near the midpoint of the activation curve) by 51 ± 7%. When applied after inhibition by grammotoxin, however, somatostatin had no additional effect. Tail current after a step to +80 mV (near the midpoint of the activation curve in the presence of toxin) was inhibited only 1 ± 4% compared with the inhibition by grammotoxin alone (six cells; same cell preparations in which the effect of somatostatin alone was assayed).

Discussion

Inhibition of N- and P-type channels. On the basis of occlusion experiments with ω-conotoxin-GVIA and ω-Aga-IVA, Piser *et al.* (16) proposed that grammotoxin targeted both N- and P-type calcium channels in hippocampal neurons, which have multiple types of calcium channels; the same conclusion was reached from experiments in which calcium entry into brain synaptosomes and synaptic transmission were examined (20). Our experiments on Purkinje neurons, which have predominantly P-type current, and sympathetic neurons, which have predominantly N-type current, offer strong support for the conclusion that grammotoxin potently inhibits both N- and P-type channels.

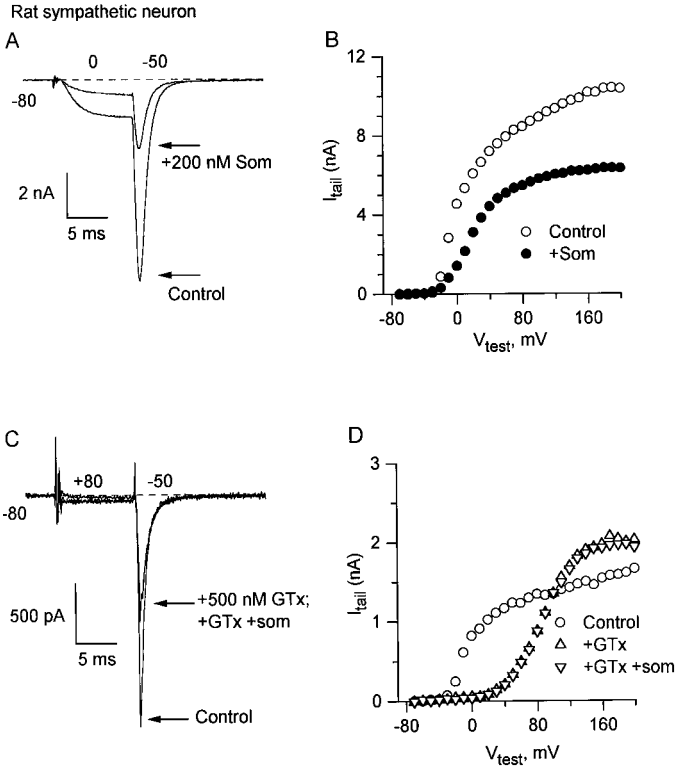

Fig. 12. Effects of somatostatin (*Som*) on N-type channels from rat SCG neurons at 22° with and without grammotoxin (*GTx*). A, Effect of 200 nM somatostatin on current evoked by a 10-msec step to 0 mV, with tail current at −50 mV. B, Tail current as a function of test voltage in control (○) and 200 nM somatostatin (●). C, Effect of 200 nM somatostatin after maximal inhibition by 500 nM grammotoxin on tail current at −50 mV evoked by a 10-msec step to +80 mV (different cell from that used for A and B). The tail currents in grammotoxin and grammotoxin plus somatostatin superimpose. The pulse to +80 does not evoke outward currents because TEA is used as the main internal cation. D, Tail current as a function of test voltage in control (○), 500 nM grammotoxin (△), and 500 nM grammotoxin plus 200 nM somatostatin (▽). The internal solution consisted of 117 mM TEA-Cl, 4.5 mM $MgCl_2$, 9 mM EGTA, 9 mM HEPES, 14 mM creatine phosphate (Tris salt), and 0.3 mM GTP (Tris salt), pH 7.4, adjusted with TEA-OH. The external solution consisted of 160 mM TEA-Cl, 10 mM HEPES, 5 mM $BaCl_2$, 0.6 μM tetrodotoxin, 1 mg/ml cytochrome *c*, and 5 μM nimodipine.

We find that the inhibition of both P- and N-type channels results from a large depolarizing shift in the gating of the channels. The modification of gating by grammotoxin is very similar for N- and P-type channels, even quantitatively. Measured with short (10–15 msec) test pulses, the voltage for half-maximal activation increased ≈+110 mV for P-type channels and ≈+100 mV for N-type channels. The slope of the Boltzmann fit to activation curves became shallower for both channels. For both channel types, currents elicited by large depolarizations in the presence of toxin activated more slowly and often were larger than in control. The nearly identical mechanism of action on the two types of channels suggests that the binding site (or sites) for grammotoxin may be very similar on the two types of channels. Preliminary results indicate that grammotoxin alters cloned α_{1A} but not α_{1C} calcium channel gating in a manner similar to the alteration of native P- and N-type channel gating.[1] The differences between different cloned channels should provide a starting point for locating the grammotoxin binding site.

Mechanism and state dependence of grammotoxin inhibition. Grammotoxin binds with high affinity to N- and P-type calcium channels at normal resting potentials with channels in the closed state; complete inhibition was seen for concentrations of >50 nM when assayed with depolarizations to near the peak of the current-voltage relation. For both channel types, channels can still pass current in the presence of toxin when subjected to very large depolarizations. This is most simply interpreted as opening of channels that remain toxin bound. The experiments with grammotoxin block of monovalent-carried inward and outward currents (Fig. 9) suggest that the crucial element is voltage, not the current-carrying ion or the direction of current flow. The simplest interpretation is that grammotoxin binds with high affinity to closed, resting states of the channel and that bound toxin makes it more difficult for channels to be opened by depolarization, so much larger depolarizations are required for channel activation. There is a reciprocal interaction between channel gating and toxin binding, so activated channels have lower affinity for toxin and toxin unbinds much faster than from resting channels.

This picture of an allosteric action of toxin in stabilizing closed states of the channel is essentially identical to the interpretation of effects of ω-Aga-IVA on P-type calcium channels (13) and hanatoxin on the *drk1* K channel (14). The modulation of voltage-dependent sodium channels by α-scorpion toxins has been interpreted in the same way but with one important difference: binding to both resting and open channels is tight, whereas binding to inactivated channels is weak (11, 31–33). As a result, α-scorpion toxins inhibit inactivation of the channels rather than activation, so channel activity is enhanced rather than depressed. However, just as for grammotoxin, large depolarizations induce faster unbinding of α-scorpion toxin, in this case by driving channels into

[1] F. Noceti, S. I. McDonough, L. Birnbaumer, E. Stefani, and B. P. Bean, unpublished observations.

a low affinity inactivated state rather than an open state. The state dependence of scorpion toxin binding was originally revealed by direct measurement of changes of radiolabeled toxin binding affinity on membrane depolarization by KCl (34); such measurements may be possible for grammotoxin binding, although the acceleration of unbinding requires depolarization far beyond 0 mV to be maximal (Fig. 11).

Mutagenesis experiments have shown that residues in the S3–S4 loop of domain IV of the channel participate in binding of α-scorpion toxin binding (33). Hanatoxin binding to *drk1* potassium channels can also be greatly diminished by mutation of residues on the S3–S4 linker of the channel (14, 35). Because grammotoxin is a highly hydrophilic molecule, it, too, must interact with extracellular loops of the calcium channel. It will be interesting to see whether its sites of interaction are analogous to those of α-scorpion toxins or hanatoxin. A possible mechanism for a toxin-induced shift in the voltage dependence of activation is an electrostatic repulsion between a positively charged toxin molecule bound to the outside of the channel and the positively charged residues in the S4 region believed to be responsible for voltage-dependent channel gating; this is the interpretation given for effects of a mutated μ-conotoxin on gating of skeletal muscle sodium channels (shift by +6 mV in the midpoint) (36). It is very doubtful that such a mechanism is responsible for the much larger changes in gating seen with grammotoxin or ω-Aga-IVA, especially because comparably large voltage-dependent effects on P-type channels are seen with cationic ω-Aga-IVA (net charge = +7) and with the variant ω-Aga-IVB, which has no net charge (37, 38).

The dissociation rate of toxin is enhanced by channel activation, as inferred by the ability of multiple strong depolarizations to accelerate recovery of current after toxin has been removed from the bathing solution. The rate of dissociation saturated at $\approx$4 sec^{-1} for voltages positive to +120 mV, and the voltage dependence of the dissociation rate was comparable to the voltage dependence of channel activation (Fig. 11). The saturation implies that the voltage dependence of toxin dissociation derives from a dependence on channel gating state and not from an intrinsic voltage dependence of toxin binding or displacement by permeating ions. The saturating rate of dissociation (4 sec^{-1} for $>$+150 mV at 22°) is far too slow to account for the kinetics of channel opening at large depolarizations in the presence of toxin; this occurs with an apparent rate constant of $\approx$100–200 sec^{-1} at voltages of +150–180 mV (10°; Figs. 2–4). The comparison supports the interpretation that toxin is still bound when channels open with large depolarizations. Toxin then unbinds from open channels on a much slower time scale (but the unbinding is much faster than that from channels in the closed state).

In many cells, grammotoxin substantially enhanced the current elicited by very large depolarizations; this was true for both P- and N-type channels. Although it is possible that the effect reflects an increase in single-channel conductance, it seems more likely that it results from an enhanced probability of channel opening. The magnitude of the increase varied considerably from cell to cell, which can easily be rationalized if the maximal probability of being open under control conditions varied from cell to cell. It seems less likely that single-channel conductance or a modification would vary from cell to cell. There have been no single-channel recordings of either N- or P-type channel activity at the strong depolarizations relevant to this effect ($>$+100 mV), so it is difficult to guess how grammotoxin may alter channel gating so as to enhance open probability. At lower depolarizations, both P- and N-type channels show flickering-like openings (39, 40), as if there were rapid transitions between the open state and a closed state. Possibly, grammotoxin stabilizes the open state, reduces the flickering, and produces an increased probability of being open.

Comparison with ω-Aga-IVA. The inhibition of P-type channels by grammotoxin shares many mechanistic features with inhibition of P-type channels by the *A. aperta* toxin ω-Aga-IVA (13, 17). Both toxins increase the voltage required for channel opening, slow channel activation, and seem to have lower affinity for activated channels because trains of large depolarizations remove inhibition independent of outward current flow. The estimated equilibrium shift in half-maximal activation voltage is $\approx$+40 mV for both toxins; the activation slope is similar; and the k_{off} value for grammotoxin at +150 mV from P-type channels of 3.7 sec^{-1} (calculated from Fig. 6) is essentially the same as that measured for ω-Aga-IVA. However, grammotoxin slows P-type channel activation much more than ω-Aga-IVA at all voltages. At +90 mV, P-type channels activate with time constant τ of 1.4 msec in control, τ of 3.7 msec in ω-Aga-IVA (13), and τ of 49 msec in grammotoxin (Fig. 5). The $>$+100-mV shift in half-maximal activation voltage by grammotoxin as measured from rest with short test pulses is in large part due to this kinetic slowing. We were able to make use of the additional slowing of activation kinetics as well as the altered voltage dependence to show that grammotoxin binding is not prevented by saturating ω-Aga-IVA exposure. Thus grammotoxin binds to different or additional sites than ω-Aga-IVA; the P-type calcium channel may have multiple toxin binding sites, as found for sodium channels (9–12). We have no direct evidence for multiple binding sites for grammotoxin, but on washout of toxin, recovery of P-type current occurred with complex, non-exponential kinetics, which is consistent with multiple binding sites. An interesting possibility is that ω-Aga-IVA affects gating of one pseudosubunit of the channel and that grammotoxin affects the gating of multiple subunits.

Comparison with G protein inhibition. The altered voltage dependence of channels with grammotoxin and the unbinding of grammotoxin with strong depolarization are similar to inhibitory effects of G proteins on native and cloned calcium channels. It is very unlikely that the similarity reflects common binding sites because G proteins act from within the cell and grammotoxin acts from outside the cell. Most likely, the similarity results from a common allosteric mechanism of action: both stabilize closed states of the channel. If the G proteins activated by somatostatin act at a binding site distinct from the grammotoxin binding site, it initially seems somewhat surprising that somatostatin had no effect on grammotoxin-modified channels. One possibility is that $\beta\gamma$ subunits and grammotoxin affect the gating movement of different pseudosubunits and grammotoxin causes a large shift of gating of one pseudosubunit, which effectively becomes limiting for channel opening. Thus, a smaller $\beta\gamma$ -induced shift in gating of another pseudosubunit might have no effect on the overall voltage dependence of opening.

References

1. Aiyar, J., J. M. Withka, J. P. Rizzi, D. H. Singleton, G. C. Andrews, W. Lin, J. Boyd, D. C. Hanson, M. Simon, B. Dethlefs, C.-I. Lee, J. E. Hall, G. A. Gutman, and K. G. Chandy. Topology of the pore-region of a K^+ channel revealed by the NMR-derived structures of scorpion toxins. *Neuron* **15:** 1169–1181 (1996).
2. Naranjo, D., and C. Miller. A strongly interacting pair of residues on the contact surface of charybdotoxin and a shaker K^+ channel. *Neuron* **16:** 123–130 (1996).
3. Ranganathan, R., J. H. Lewis, and R. MacKinnon. Spatial localization of the K^+ channel selectivity filter by mutant cycle-based structure analysis. *Neuron* **16:**131–139 (1996).
4. MacKinnon, R., and C. Miller. Mutant potassium channels with altered binding of charybdotoxin, a pore-blocking peptide inhibitor. *Science (Washington D. C.)* **245:**1382–1385 (1989).
5. Noda, M., H. Suzuki, S. Numa, and W. Stuhmer. A single point mutation confers tetrodotoxin and saxitoxin insensitivity on the sodium channel II. *FEBS Lett.* **259:**213–216 (1989).
6. Kontis, K. J., and A. I. Goldin. Site-directed mutagenesis of the putative pore region of the rat IIA sodium channel. *Mol. Pharmacol.* **43:**635–644 (1993).
7. Lipkind, G. M., and H. A. Fozzard. A structural model of the tetrodotoxin and saxitoxin binding site of the Na^+ channel. *Biophys. J.* **66:**1–13 (1994).
8. Schlief, T., R. Schonherr, and K. Imoto. Pore properties of rat brain II sodium channels mutated in the selectivity filter domain. *Eur. Biophys. J.* **25:**75–91 (1996).
9. Catterall, W. A. Neurotoxins that act on voltage-sensitive sodium channels in excitable membranes. *Annu. Rev. Pharmacol. Toxicol.* **20:**15–43 (1980).
10. Hille, B. *Ionic Channels of Excitable Membranes*. Sinauer Associates, Sunderland, MA (1992).
11. Strichartz, G. R., T. Rando, and G. K. Wang. An integrated view of the molecular toxinology of sodium channel gating in excitable cells. *Annu. Rev. Neurosci.* **10:**237–267 (1987).
12. Catterall, W. A. Structure and function of voltage-gated ion channels. *Annu. Rev. Biochem.* **64:**493–531 (1995).
13. McDonough, S. I., I. M. Mintz, and B. P. Bean. Alteration of P-type calcium channel gating by the spider toxin ω-Aga-IVA. *Biophys. J.* **72:**2117–2128 (1997).
14. Swartz, K. J., and R. MacKinnon. Hanatoxin modifies the gating of a voltage-dependent K^+ channel through multiple binding sites. *Neuron* **18:**665–673 (1997).
15. Lampe, R. A., P. A. DeFeo, M. D. Davison, J. Young, J. L. Herman, R. C. Spreen, M. B. Horn, T. M. Mangano, and R. A. Keith. Isolation and pharmacological characterization of ω-grammotoxin SIA, a novel peptide inhibitor of neuronal voltage-sensitive calcium channel responses. *Mol. Pharmacol.* **44:**451–460 (1993).
16. Piser, T. M., R. A. Lampe, R. A. Keith, and S. A. Thayer. ω-Grammotoxin SIA blocks multiple, voltage-gated, Ca^{2+} channel subtypes in cultured rat hippocampal neurons. *Mol. Pharmacol.* **48:**131–139 (1995).
17. Mintz, I. M., M. E. Adams, and B. P. Bean. P-type calcium channels in rat central and peripheral neurons. *Neuron* **9:**1–20 (1992).
18. Boland, L. M., J. A. Morrill, and B. P. Bean. ω-Conotoxin block of N-type calcium channels in frog and rat sympathetic neurons. *J. Neurosci.* **14:** 5011–5027 (1994).
19. Hamill, O. P., A. Marty, E. Neher, B. Sakmann, and F. J. Sigworth. Improved patch-clamp techniques for high-resolution current recording from cells and cell-free membrane patches. *Pflueg. Arch. Eur. J. Physiol.* **391:**85–100 (1981).
20. Keith, R. A., T. J. Mangano, R. A. Lampe, P. A. DeFeo, M. J. Hyde, and B. A. Donzanti. Comparative actions of synthetic *omega*-grammotoxin SIA and synthetic *omega*-Aga-IVA on neuronal calcium entry and evoked release of neurotransmitters in vitro and in vivo. *Neuropharmacology* **34:** 1515–1528 (1995).
21. Piser, T. M., R. A. Lampe, R. A. Keith, and S. A. Thayer. ω-Grammotoxin blocks action-potential-induced Ca^{2+} influx and whole-cell Ca^{2+} current in rat dorsal-root ganglion neurons. *Pflueg. Arch. Eur. J. Physiol.* **426:**214–220 (1994).
22. Ikeda, S. R. Double-pulse calcium channel current facilitation in adult rat sympathetic neurons. *J. Physiol.* **439:**181–214 (1991).
23. Bean, B. P. Neurotransmitter inhibition of neuronal calcium currents by changes in channel voltage dependence. *Nature (Lond.).* **340:**153–156 (1989).
24. Elmslie, K. S., W. Zhou, and S. W. Jones. LHRH and GTP-γ-S modify calcium current activation in bullfrog sympathetic neurons. *Neuron* **5:** 75–80 (1990).
25. Kuo, C.-C., and B. P. Bean. G-protein modulation of ion permeation through N-type calcium channels. *Nature (Lond.)* **365:**258–262 (1993).
26. Boland, L. M., and B. P. Bean. Modulation of N-type calcium channels in bullfrog sympathetic neurons by luteinizing hormone-releasing hormone: kinetics and voltage dependence. *J. Neurosci.* **13:**516–533 (1993).
27. Ikeda, S. R. Voltage-dependent modulation of N-type calcium channels by G-protein βγ subunits. *Nature (Lond.)* **380:**255–258 (1996).
28. Patil, P. G., M. de Leon, R. R. Reed, S. Dubel, T. P. Snutch, and D. T. Yue. Elementary events underlying voltage-dependent G-protein inhibition of N-type calcium channels. *Biophys. J.* **71:**2509–2521 (1996).
29. Carabelli, V., M. Lovallo, V. Magnelli, H. Zucker, and E. Carbone. Voltage-dependent modulation of single N-type Ca^{2+} channel kinetics by receptor agonists in IMR32 cells. *Biophys. J.* **70:**2144–2154 (1996).
30. Shapiro, M. S., and B. Hille. Substance P and somatostatin inhibit calcium channels in rat sympathetic neurons via different G protein pathways. *Neuron* **10:**11–20 (1993).
31. Mozhayeva, G. N., A. P. Naumov, E. V. Grishin, and N. M. Soldatov. Potential-dependent interaction of toxin from venom of the scorpion *Buthus eupeus* with sodium channels in myelinated fibre. *Biochim. Biophys. Acta* **597:**587–602 (1980).
32. Strichartz, G. R., and G. K. Wang. Rapid voltage-dependent dissociation of scorpion α-toxins coupled to Na channel inactivation in amphibian myelinated nerves. *J. Gen. Physiol.* **88:**413–435 (1986).
33. Rogers, J. C., Y. Qu, T. N. Tanada, T. Scheuer, and W. A. Catterall. Molecular determinants of high affinity binding of α-scorpion toxin and sea anemone toxin in the S3–S4 extracellular loop in domain IV of the Na^+ channel α subunit. *J. Biol. Chem.* **271:**15950–15962 (1996).
34. Catterall, W. A. Membrane-potential dependent binding of scorpion toxin to the action potential Na^+ ionophore. *J. Biol. Chem.* **252:**8660–8668 (1977).
35. Swartz, K. J., and R. MacKinnon. Mapping the receptor site for hanatoxin, a gating modifier of voltage-dependent K^+ channels. *Neuron* **18:**675–682 (1997).
36. French, R. J., E. Prusak-Sochaczewski, G. W. Zamponi, S. Becker, A. S. Kularatna, and R. Horn. Interactions between a pore-blocking peptide and the voltage sensor of the sodium channel: an electrostatic approach to channel geometry. *Neuron* **16:**407–413 (1996).
37. Mintz, I. M., V. J. Venema, K. Swiderek, T. Lee, B. P. Bean, and M. E. Adams. P-type calcium channels blocked by the spider toxin ω-Aga-IVA. *Nature (Lond.).* **355:**827–829 (1992).
38. Adams, M. E., I. M. Mintz, M. D. Reily, V. Thanabal, and B. P. Bean. Structure and properties of ω-agatoxin IVB, a new antagonist of P-type calcium channels. *Mol. Pharmacol.* **44:**681–688 (1993).
39. Elmslie, K. S. Identification of the single channels that underlie the N-type and L-type calcium currents in bullfrog sympathetic neurons. *J. Neurosci.* **17:**2658–2668 (1997).
40. Usowicz, M. M., M. Sugimori, B. Cherksey, and R. Llinas. P-type calcium channels in the somata and dendrites of adult cerebellar Purkinje cells. *Neuron* **9:**1185–1199 (1992).

Send reprint requests to: Dr. Stefan I. McDonough, Department of Neurobiology, Harvard Medical School, 220 Longwood Avenue, Boston, MA 02115.